Techno-Science Research Journal 7 (2019) 64-68

Content list available at ITC

Techno-Science Research Journal

Journal Homepage : www.itc.edu.kh

Techno-Science Research Journal

Dynamic Modeling for a Multi Rigid-Body Unmanned Aerial Vehicle

Sarot Srang

Department of Industrial and Mechanical Engineering, Institute of Technology of Cambodia, Russian Federation Blvd., P.O. Box 86, Phnom Penh, Cambodia.

Abstract: *This work proposes an effective and efficient use of energy supply for a Vertical Take-Off and Landing Unmanned Aerial Vehicle (VTOL UAV). Because of low power consumption, a 2-DOF parallel mechanism is used as dual axis solar tracker, and mounted on a UAV. Then, the UAV becomes a multi rigid-body UAV which has loops of connected links. Dynamic modeling for the system is one of the most challenging engineering problems. To deal with it, kinematic constraints of all joints are determined. Undetermined close form reaction forces at joints are obtained from the kinematic constraints. Using Newton's method, dynamic equation for each body exerted by external forces and reaction forces is formulated. A fully determined equation, which is system equation of algebraic-differential equations, is obtained by appending kinematic and dynamic equations. For both kinematic and dynamic equations, Cartesian coordinate and Euler parameter are used to describe translation and rotation motions respectively.*

Keywords: Unmanned Aerial Vehicles, Parallel mechanism, Dynamic Modeling, Multi-Rigid Body

1. INTRODUCTION

Effective and efficient energy supply by solar energy to power UAVs has been an active research for more than four decades. The first solar-powered UAV, Sunrise I of Astro Flight Inc., took its first flight in California in 1974, [1]. In 2003, possible use of a solar-powered UAV for agricultural decision support was reported by [2]. In [3], continuous flight of solar-powered airplanes was considered, and a methodology used for the complete design was presented. With a mechanism simulating the motion of aircraft, virtual flight system was designed for evaluation of a solar-powered UAV by [4]. For improving efficiency of solar energy collection, a UAV with onboard solar tracking system was designed and constructed by [5]. In our work, we specifically study this type of design for the purpose of effective and efficient use of energy supply. Literally, single and dual axis solar trackers are the systems that improve energy efficiency by optimizing collection of sun light onto solar panel. In [5], a single-axis solar tracker was designed and tested. The tracking system autonomously rotated an onboard solar panel to find the angle of maximum solar irradiance while the UAV was found to have the maximum and minimum of net energy gain over a conventional solar-powered UAV of 34.5% and 0.8% respectively.

This material is based upon work supported by the Air Force Office of Scientific Research under award number FA2386-17-1-0148

* Coresponding authors:
E-mail: srangsarot@itc.edu.kh; Tel: +855-85-689-858;

Dual axis solar tracker has been of interest research topic for many researchers, [6]-[19], because of its outperformance over single axis solar tracker. Many researches on energy gain from solar tracking systems compared to tilted fixed panel had been done both theoretically and experimentally [6]. Energy gain from a single axis solar tracker was reported to be 20% [17] while energy gain from a dual axis solar tracker was 30-40% [18]. [19] proposed a two-axis decoupled solar tracking system based on parallel mechanism and showed that the tracker requires less driving torque, thus less power dissipation than the conventional serial tracker does. Furthermore, the tracking system does not need reducer with large reduction ratio, which reduce it weight. In our study, we use this tracking system onboard, and we consider VTOL UAV. The complete system is called a multi rigid-body UAV, and, thus, its dynamic modeling is challenging.

In general, dynamic modeling using Lagrange's dynamic equation yields the smallest number of differential equations and, therefore, computational efficient. However, the order of nonlinearity is high, and derivation of equation in expanded form of multibody system with loops of connected links is very tedious. For a system with more than one loop like the tracker, the derivation is even more difficult, and only partial reaction forces can be determined. With Cartesian coordinates and Euler parameter for describing rotation, dynamic modeling using Newton-Euler's method is much simpler, and systematic generation of kinematic constraints of kinematic pairs and dynamic equations can be

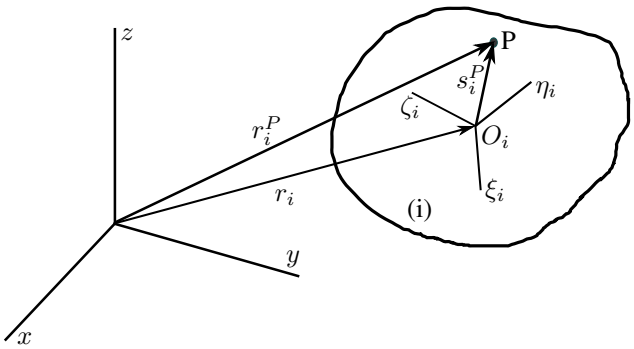

Fig. 1. Cartesian coordinate system

derived easily, [20]. The method yields system equations of algebraic-differential equations. Reaction forces and the coordinates describing motion of a system are obtained from solving the equations. The reaction force has an advantage for mechanical structure design. However, the analysis of reaction forces is out of scope of this work. With the support of increasing computational power of computer nowadays, we use this method for modeling which is easy to use for simulation.

The remaining contents in this paper are organized as follows. In section II, the parallel mechanism is explained on configuration and degree of freedom, and its kinematic is described by using Cartesian coordinate. Dynamic equations for unconstrained and constrained body which are described in Cartesian coordinate and using Euler parameter are given in section III. For constrained body, the resulted equation is in the form of system algebraic-differential equations. In section IV, the dynamic modeling of the multi rigid-body UAV is elaborated. The final section sums up our work.

II. Kinematic equations for the mechanism

Cartesian coordinate is used to describe the system configuration, and constraint equations are obtained from individual joints. Figure 1 shows the coordinate system, where $(Oxyz)$ is global frame and $(O_i\xi_i\eta_i\zeta_i)$ is body-fixed frame attached on body i with the center of mass O_i. A point P on the body has coordinate as a vector in body-fixed frame and global frame defined by s_i^P and r_i^P respectively.

Figure 2 shows a parallel mechanism which is used as dual axis solar tracker. The body numbers are labeled as seen in the figure. The mechanism consists of 7 connected rigid bodies. It has a global coordinate $(Oxyz)$, and each body has its own body-fixed frame as explained in Fig. 1. Body 7 is connected with body 5 and 6 via 2 spherical joints and with body 4 via a universal joint. Body 6 is connected with body 2 via a revolute joint. Body 5 is connected to body 3 via a universal joint. Body 4 is connected to body 1 (ground) via another revolute joint. Body 3 is connected with body 1 via a translational joint. Body 2 is connected with body 1 via another translational joint. Two linear actuators are attached at the translational joints. The actuators exert forces on body 2 and 3 along vertical axes.

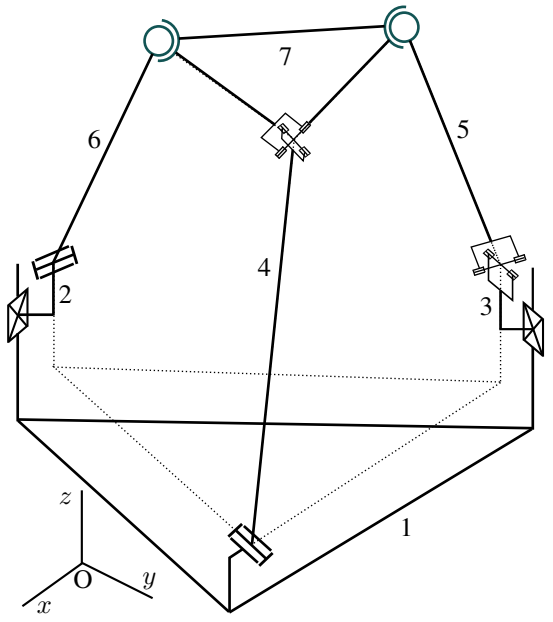

Fig. 2. Parallel Mechanism

Degree of Freedom (DOF) of a system is the minimum number of coordinates required to fully describe the configuration of the system. DOF for spatial mechanism can be defined by

$$DOF = 6(b-1) - \sum_{k \in T_j} n_k c_k \tag{1}$$

where b is the number of the body; n_k is the number of each type of joints; c_k is the number of constraints for each type of joints; and TJ is the set of types of joints. For the parallel mechanism shown in Fig. 2, denote S, U, R and T as spherical joint, universal joint, revolute joint, and translational joint, respectively. Then, we have $b = 7$, $TJ = \{\text{S,U,R,T}\}$, $n_{k \in TJ} = \{2, 2, 2, 2\}$, and $c_{k \in TJ} = \{3, 4, 5, 5\}$. Therefore DOF can be calculated as

$$DOF = 6(7-1) - 2 \times 3 - 2 \times 4 - 2 \times 5 - 2 \times 5 = 2$$

Denote

- $q_i = [r^T, p^T]_i^T = [x, y, z, e_0, e_1, e_2, e_3]_i^T$ a coordinate vector of the body i, where r_i is position vector of the center of mass of the body as illustrated in Fig. 1, and $p_i = [e_0, e^T]_i^T = [e_0, e_1, e_2, e_3]_i^T$ is Euler parameter. The parameter satisfies a mathematical relationship,

$$p_i^T p_i - 1 = 0. \tag{2}$$

The second time derivative of the equation is

$$p_i^T \ddot{p}_i + \dot{p}_i^T \dot{p}_i = 0 \tag{3}$$

- R_i a rotational matrix of body i, and a pair of 3×4 matrices G_i and L_i defined as $G_i = [-e, \tilde{e} + e_0 I]_i$ and $L_i = [-e, -\tilde{e} + e_0 I]_i$. Then $R_i = G_i L_i^T$, [20]. The

global coordinate of the point P illustrated in Fig. 1 can be defined by

$$r_i^P = r_i + R_i s_i'^P = r_i + G_i L_i^T s_i'^P, \tag{4}$$

where $s_i'^P = [\xi^P, \eta^P, \zeta^P]_i^T$ is body-fixed coordinate of the point P.

- $q = [q_1^T, q_2^T, q_3^T, q_4^T, q_5^T, q_6^T, q_7^T]^T$ coordinate vector for describing the configuration of the mechanism, and its respective first and second time derivative, $\dot{q}$ and $\ddot{q}$, for describing the motion of the mechanism. The number of coordinates of the system is $n = 7 \times 7 = 49$, and the number of Euler parameter relationship (or mathematical constraint) is 7.
- and

$$\Phi \equiv \Phi(q) = 0 \tag{5}$$

kinematic equation derived from kinematic constraints which have 34 equations. The compact form of the kinematic equation for each joint is given in Appendix A.

III. Dynamic equations for unconstrained and constrained bodies

From Newton's method, an unconstrained body i with mass m_i and moment of inertia J_i' with respect to its center of mass exerted by external force f_i and moment τ_i' has dynamic equation of motion as

$$\begin{bmatrix} N & 0 \\ 0 & J' \end{bmatrix}_i \begin{bmatrix} \ddot{r} \\ \dot{\omega}' \end{bmatrix}_i + \begin{bmatrix} 0 \\ \tilde{\omega}' J' \omega' \end{bmatrix}_i = \begin{bmatrix} f \\ \tau' \end{bmatrix}_i, \tag{6}$$

where $N_i = \text{diag}([m\ m\ m])_i$ and ω_i' is angular velocity defined in the body-fixed frame. To use Euler parameters, the rotation equation of (6) is transformed and appended with (3) as

$$\begin{bmatrix} 2J'L \\ p^T \end{bmatrix}_i \ddot{p}_i + \begin{bmatrix} LH \\ \dot{p}^T \end{bmatrix}_i \dot{p}_i = \begin{bmatrix} \tau' \\ 0 \end{bmatrix}_i, \tag{7}$$

where $H_i = 4\dot{L}_i^T J_i' L_i$.

A constrained body i is additionally exerted by reaction forces and moments $[f^{(c)}, \tau'^{(c)}]_i^T$ from joints. These forces and moments can be transformed to coordinate system consistent with q denoted by $[f^{*(c)}, \tau^{*(c)}]_i^T$ and defined by

$$\begin{bmatrix} f^{*(c)} \\ \tau^{*(c)} \end{bmatrix}_i = \begin{bmatrix} \Phi_r^T \\ \Phi_p^T \end{bmatrix}_i \lambda, \tag{8}$$

where $\lambda = [\lambda_1, \ldots, \lambda_{34}]$ is called Lagrange multiplier, and $[\Phi_r, \Phi_p]_i = \Phi_{q_i}$ is Jacobian matrix of the kinematic constraint $\Phi \equiv \Phi(q)$ with respect to q_i. To be used with the formulation (7), the moment in (8) is transformed to be

$$\begin{aligned} \tau'^{(c)} &= \frac{1}{2} L_i \tau'^{*(c)} \\ &= \frac{1}{2} L_i \Phi_{p_i}^T \lambda, \end{aligned}$$

then first equation of (7) for constrained body becomes

$$2J' L_i \ddot{p}_i + L_i H_i \dot{p}_i - \frac{1}{2} L_i \Phi_{p_i}^T \lambda = \tau_i'. \tag{9}$$

For the system with 7 bodies, the dynamic equation can be obtained as

$$\begin{bmatrix} M & B^T \\ P & 0 \end{bmatrix} \begin{bmatrix} \ddot{q} \\ -\lambda \end{bmatrix} + \begin{bmatrix} c_1 \\ c_2 \end{bmatrix} = \begin{bmatrix} g \\ 0 \end{bmatrix}, \tag{10}$$

where

$$M = \begin{bmatrix} N_1 & 0 & \ldots & 0 & 0 \\ 0 & 2J_1' L_1 & \ldots & 0 & 0 \\ \vdots & \vdots & \ddots & \vdots & \vdots \\ 0 & 0 & \ldots & N_7 & 0 \\ 0 & 0 & \ldots & 0 & 2J_7' L_7 \end{bmatrix},$$

$$B = [\Phi_{r_1}, \frac{1}{2}\Phi_{p_1} L_1^T, \ldots, \Phi_{r_7}, \frac{1}{2}\Phi_{p_7} L_7^T],$$

$$P = \begin{bmatrix} 0^T & p_1^T & \ldots & 0^T & 0^T \\ \vdots & \vdots & \ddots & \vdots & \vdots \\ 0^T & 0^T & \ldots & 0^T & p_7^T \end{bmatrix},$$

$$c_1 = \begin{bmatrix} 0 \\ L_1 H_1 \dot{p}_1 \\ \vdots \\ 0 \\ L_7 H_7 \dot{p}_7 \end{bmatrix},\ c_2 = \begin{bmatrix} \dot{p}_1^T \dot{p}_1 \\ \vdots \\ \dot{p}_7^T \dot{p} \end{bmatrix},\ \text{and } g = \begin{bmatrix} f_1 \\ \tau_1' \\ \vdots \\ f_7 \\ \tau_7' \end{bmatrix}$$

To solve this equation for q and λ, the constraint equation is needed. The second time derivative of the constraint equation (5) is given by

$$\Phi_q \ddot{q} = \gamma, \tag{11}$$

where $\gamma = -(\Phi_q \dot{q})_q \dot{q}$ is called the right-hand-side of acceleration equation. This equation is then appended with (10) to yield a system of algebraic-differential equation as

$$\begin{bmatrix} M & B^T \\ P & 0 \\ \Phi_q & 0 \end{bmatrix} \begin{bmatrix} \ddot{q} \\ -\lambda \end{bmatrix} + \begin{bmatrix} c_1 \\ c_2 \\ 0 \end{bmatrix} = \begin{bmatrix} g \\ 0 \\ \gamma \end{bmatrix}, \tag{12}$$

IV. Dynamic equations for parallel-mechanism-mounted UAV

Figure 3 shows the combined system of an hexacopter and the parallel mechanism. Body numbers are labeled as illustrated in the figure. Body-fixed frame for the hexacopter (body 1) is attached at the center of mass of the body.

Thrust and torque generated by a propeller are modeled as

$$f_k = [0, 0, K_f \omega_k^2]^T, \tag{13}$$

$$\tau_k = [0, 0, -\text{sign}(\omega_k) K_\tau \omega_k^2]^T \tag{14}$$

where $k = 1, \ldots, 6$, K_f and K_τ are force and torque constants respectively, and ω_k is angular velocity of the k-th propeller. Let a control input vector generated by the propellers,

$$u_p = [u_1, \ldots, u_6]^T = [\omega_1^2, \ldots, \omega_6^2]^T. \tag{15}$$

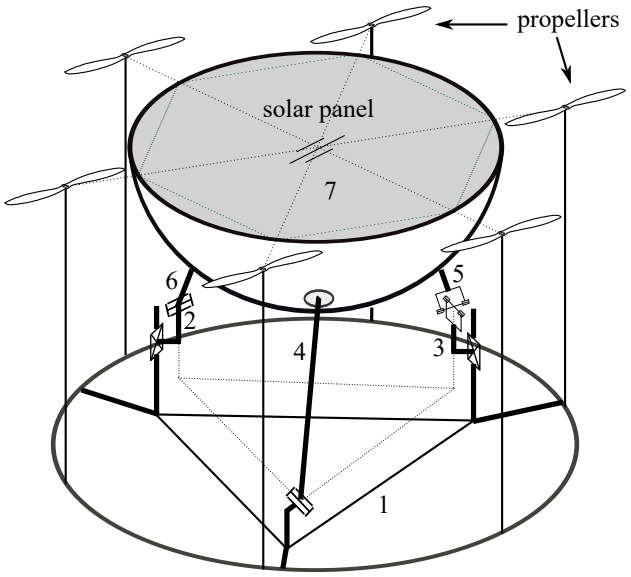

Fig. 3. Parallel-mechanism-mounted UAV

Then, the total force and moment generated by all the propellers are

$$\begin{aligned} f_p &= \sum_k f_k = A_{pf} u_p \\ \tau_p &= \sum_k (\tilde{a}_k f_k + \tau_k) = A_{p\tau} u_p \end{aligned} \tag{16}$$

where $A_{pf} = 1_z[k_f, \ldots, k_f]$,

$$A_{p\tau} = [k_f \tilde{a}_1 1_z - k_\tau \text{sign}(\omega_1) 1_z, \ldots, k_f \tilde{a}_6 1_z - k_\tau \text{sign}(\omega_6) 1_z],$$

where $1_z = [0, 0, 1]^T$, and a_k is vector from the center of mass of the hexacopter to axis of propeller k.

Two linear actuators are mounted on the hexacopter and exert forces on the body 2 and 3 through the translational joints. The forces are also control input for the system (12) and denoted by

$$\begin{bmatrix} f_{1-2,\zeta} \\ f_{1-3,\zeta} \end{bmatrix} = \begin{bmatrix} u_7 \\ u_8 \end{bmatrix} \text{ and } \begin{bmatrix} f_{2-1,\zeta} \\ f_{3-1,\zeta} \end{bmatrix} = - \begin{bmatrix} u_7 \\ u_8 \end{bmatrix}, \tag{17}$$

where u_7 and u_8 are scalars.

Denote $u = [u_p, u_7, u_8]^T$, a control input vector for the whole system. Then, the non-zero external forces and moments which exert on respective body 1, 2 and 3 are given by

$$\begin{aligned} g_1 &= \begin{bmatrix} R_1(f_p - u_7 - u_8) \\ \tau_p - \tilde{b}_1 1_z u_7 - \tilde{b}_2 1_z u_8 \end{bmatrix} = \begin{bmatrix} A_{1f} \\ A_{1\tau} \end{bmatrix} u \\ g_2 &= \begin{bmatrix} R_2 1_z u_7 \\ 0 \end{bmatrix} = \begin{bmatrix} A_{2f} \\ 0 \end{bmatrix} u \\ g_3 &= \begin{bmatrix} R_3 1_z u_8 \\ 0 \end{bmatrix} = \begin{bmatrix} A_{3f} \\ 0 \end{bmatrix} u \end{aligned} \tag{18}$$

where

$$\begin{aligned} A_{1f} &= R_1 1_z[k_f, \ldots, k_f, -1, -1], \\ A_{1\tau} &= [A_{p\tau}, -\tilde{b}_1 1_z, -\tilde{b}_2 1_z], \\ A_{2f} &= R_2 1_z[0, \ldots, 0, 1, 0], \\ A_{3f} &= R_3 1_z[0, \ldots, 0, 0, 1], \end{aligned}$$

and b_1 and b_2 are vectors from the center of mass of the hexacopter to the axes of the two linear actuators. Therefore the dynamic equation of motion (12) can be rewritten as

$$\begin{bmatrix} M & B^T \\ P & 0 \\ \Phi_q & 0 \end{bmatrix} \begin{bmatrix} \ddot{q} \\ -\lambda \end{bmatrix} + \begin{bmatrix} c_1 \\ c_2 \\ 0 \end{bmatrix} = \begin{bmatrix} 0 \\ 0 \\ \gamma \end{bmatrix} + \begin{bmatrix} A \\ 0 \\ 0 \end{bmatrix} u, \tag{19}$$

where $A = [A_{1f}^T, A_{1\tau}^T, A_{2f}^T, 0^T, A_{3f}^T, 0^T, \ldots, 0^T]^T$.

V. Conclusion

A multi rigid-body UAV consisting of a hexacopter and a parallel mechanism which is used as a dual axis solar tracker is studied. The system involves loops of connected links which induces high complexity of its kinematic and dynamic. Because of the simplicity in systematic equation generation, Cartesian coordinate and Euler parameter are used in kinematic and dynamic modelings for the parallel mechanism and the multi rigid-body UAV. The resulted dynamic model is in the form of algebraic-differential equations, which is very useful and easy to use for simulation, numerical analysis, and mechanical design. For future work, we will simulate a multi rigid-body UAV that flies and tracks the sun at same time. We will use various controllers from literature, which had been designed for single body UAV only, to observe robustness and adaptiveness of the controllers.

Appendix A

- Constraint equation for two perpendicular vectors: One constraint equation obtained from scalar product is $\Phi_{i\&j}^{(n1,1)}(q) \equiv s_i^T s_j = s_i'^T R_i^T R_j s_j' = 0$ or $\Phi_{i\&j}^{(n2,1)}(q) \equiv s_i^T d = s_i'^T R_i^T (r_j + R_j s_j'^P - r_i - R_i s_i'^P) = 0$.
- Constraint equation for two parallel vectors: Two constraint equations are obtained from cross product, $\Phi_{i\&j}^{(p1,2)}(q) \equiv \tilde{s}_i s_j = R_i \tilde{s}_i' R_i^T R_j s_j' = 0$ or $\Phi_{i\&j}^{(p2,2)}(q) \equiv \tilde{s}_i d = R_i \tilde{s}_i' R_i^T (r_j + R_j s_j'^P - r_i - R_i s_i'^P) = 0$. Although a cross product yields a vector with three components, one component is dependent of the other two components. Therefore, only two of the components are needed for obtaining constraint equations.
- Constraint equation for a common point on two bodies: Two bodies having a common point P creates three constraint equations, $\Phi_{i\&j}^{(s,3)}(q) \equiv r_i^P - r_j^P = r_i + R_i s_i'^P - r_j - R_j s_j'^P = 0$

For the parallel mechanism, by following the concept of relative constraints between two bodies from [20] the 34 constraint equations are obtained as follows:

- Spherical joint number 1 between bodies 5 and 7 has 3-constraint equations as the joint is made of two bodies

having a common point. The compact form of the equations is given by

$$\Phi_{1-3} = \Phi^{(s,3)}_{5\&7}(q) = 0 \tag{20}$$

- Spherical joint number 2 between bodies 6 and 7 also has 3-constraint equations given by

$$\Phi_{4-6} = \Phi^{(s,3)}_{6\&7}(q) = 0 \tag{21}$$

- Universal joint number 1 between bodies 4 and 7 has 4-constraint equations including 3-constraint from a common point and 1-constraint from two perpendicular vectors. Thus, the compact form of the equation for the joint is

$$\Phi_{7-10} = \begin{bmatrix} \Phi^{(s,3)}_{4\&7} \\ \Phi^{(n1,1)}_{4\&7} \end{bmatrix} = 0 \tag{22}$$

- Universal joint number 2 between bodies 3 and 5 also has 4-constraint equations given by

$$\Phi_{11-14} = \begin{bmatrix} \Phi^{(s,3)}_{3\&5} \\ \Phi^{(n1,1)}_{3\&5} \end{bmatrix} = 0 \tag{23}$$

- Revolute joint number 1 between bodies 1 and 4 has 5-constraint equations including 3-constraint from a common point and 2-constraint from two parallel vectors. Thus, the compact form of the equations is

$$\Phi_{15-19} = \begin{bmatrix} \Phi^{(s,3)}_{1\&4} \\ \Phi^{(p1,1)}_{1\&4} \end{bmatrix} = 0 \tag{24}$$

- Revolute joint number 2 between bodies 2 and 6 also has 5-constraint equations given by

$$\Phi_{20-24} = \begin{bmatrix} \Phi^{(s,3)}_{2\&6} \\ \Phi^{(p1,1)}_{2\&6} \end{bmatrix} = 0 \tag{25}$$

- Translational joint number 1 between bodies 1 and 3 has 5-constraint equations including 4-constraint from two pairs of parallel vectors and 1-constraint from two perpendicular vectors. Thus, the compact form of the equation is given by

$$\Phi_{25-29} = \begin{bmatrix} \Phi^{(p1,2)}_{1\&3} \\ \Phi^{(p2,2)}_{1\&3} \\ \Phi^{(n1,1)}_{1\&3} \end{bmatrix} = 0 \tag{26}$$

- Translational joint between bodies 1 and 2 also has 5-constraint equations given by

$$\Phi_{30-34} = \begin{bmatrix} \Phi^{(p1,2)}_{1\&2} \\ \Phi^{(p2,2)}_{1\&2} \\ \Phi^{(n1,1)}_{1\&2} \end{bmatrix} = 0 \tag{27}$$

REFERENCES

[1] R. J. Boucher, "History of solar flight," *AIIAA, SAE, and ASME, Joint Propulsion Conference,* vol. 11, no. 13, 1984.

[2] Stanley R. H., "Lolar-powered UAV mission for agricultural decision support," *International Geoscience and Remote Sensing Symposium, 2003*.

[3] A. Noth *et al.*, "Design of solar powered airplanes for continuous flight," *Autonomous Systems Laboratory*, Swiss Federal Institute of Technology Zurich, 2007.

[4] J.-S. Lee *et al.*, "Design of Virtual flight system for evaluation of solar powered UAV," *39th IEEE Annual Conference on Industrial Electronics Society*, p. 3463-3467, 2013.

[5] T. D. Tegeder, "Development of an efficient solar powered Unmanned Aerial Vehicle with an onboard solar trcker," *Brigham Young University*, 2007.

[6] H. Mousazadeh *et al.*, "A review of principle and sun-tracking methods for maximizing solar systems output," *Journal of Renewable and Sustainable Energy Reviews, Elsevier*, vol. 13, no. 8, p. 1800-1818, 2009.

[7] Y. Yao *et al.*, "A multipurpose dual-axis solar tracker with two tracking strategies," *Journal of Renewable Energy, Elsvier*, vol. 72, p. 88-98, 2014.

[8] T.-S. Zhan, "Design and implementation of the dual-axis solar tracking system," *IEEE 37th Annual Computer Software and Applications Conference*, p. 276-277, 2013.

[9] M. Zolkapli *et al.*, "High-efficiency dual-axis solar tracking development using Arduino," *IEEE International Conference on Technology, Informatics, Management, Engineering & Environment*, 2013.

[10] Y. S. S. Satish *et al.*, "Modeling and simulation of PV panel with implementation of dual-axis sun tracker," *IEEE International Conference on Electrical, Electronics, Signals, Communication and Optimization*, p. 1-5, 2015.

[11] A. Nadjah *et al.*, "New design of dual axis sun tracker with DSPIC microcontroller," *16th IEEE International Power Electronics and Motion Control Conference and Exposition*, 2014.

[12] H. Fathabadi, "Novel online sensorless dual-axis sun tracker," *IEEE/ASME Transactions on Mechatronics*, vol. 22, no. 1, p. 321-328, 2017.

[13] P. N. Vasantha *et al.*, "Space optimization and backtracking for dual axis solar photovoltaic tracker," *IEEE International WIE Conference on Electrical and Computer Engineering*, p. 451-454, 2015.

[14] A. Rhif, "A position control review for a photovoltaic system: Dual axis sun tracker," *IETE Technical Review, Taylor & Francis*, vol. 28, no. 6, p. 479-485, 2011.

[15] C. Alexandru and C. Pozna, "Simulation of a dual-axis solar tracker for improving the performance of a photovoltaic panel," *Journal of Power and Energy*, 2010.

[16] C. Alexandru and C. Pozna, "Virtual prototype of a dual-axis tracking system used for photovoltaic panels," *IEEE International Symposium on Industrial Electronics*, p. 1598-1603, 2008.

[17] M. Stern *et al.*, "Development of a low-cost integrated 20-kW-AC solar tracking sub-array for grid-connected PV power system applications," *Final Technical Report. NRELISR-520-2475 9. National Renewable Energy Laboratory, A National Laboratory of the U.S. Department of Energy nanaged by Midwest Research Institute for the U.S. Department of Energy*, 1998.

[18] Y. V. Pavel *et al.*, "Optimization of the solar energy collection in tracking and non-tracking PV solar system," *1st International Conference on Electrical and Electronics Engineering*, p. 310-314, 2004.

[19] J. Wu *et al.*, "Design and dynamics of a novel solar tracker with parallel mechanism," *IEEE/ASME Transactions on Mechatronics*, vol. 21, no. 1, p. 88-97, 2016.

[20] P. E. Nikravesh, "Computer-aided analysis of mechanical systems," *Prentice-Hall, Inc., Englewood Cliffs, New Jersey 07632*, 1988.

[21] S. Venkata *et al.*, "Attitude control of a multicopter using $\mathcal{L}_1$ augmented quaternion based backstepping," *IEEE International Conference on Aerospace Electronics and Remote Sensing Technology*, p. 170-178, 2014.